Quantitative Proteomic Profiling of Transforming Growth Factor-β1-Induced Extracellular Matrix Changes and Collagen Post-translational Modifications in primary human lung fibroblasts

Juliane Merl-Pham[a,#], Trayambak Basak[b,#], Larissa Knüppel[c], Deepak Ramanujam[d], Mark Athanason[b], Jürgen Behr[e,f], Stefan Engelhardt[d], Oliver Eickelberg[c,g], Stefanie Hauck[a], Roberto Vanacore[b,*], and Claudia A. Staab-Weijnitz[c,*]

[a] Research Unit Protein Science, Helmholtz Zentrum München, Heidemannstr. 1, 80939 Munich, Germany

[b] Center for Matrix Biology and Department of Medicine, Division of Nephrology and Hypertension, Center for Matrix Biology, Vanderbilt University Medical Center , Nashville, Tennessee 37232, United States of America

[c] Comprehensive Pneumology Center, Helmholtz-Zentrum München, Max-Lebsche-Platz 31, 81377 Munich, Germany; Member of the German Center of Lung Research (DZL)

[d] Institut für Pharmakologie und Toxikologie, Technische Universität München (TUM), Munich, Germany; DZHK (German Center for Cardiovascular Research), partner site Munich Heart Alliance, Munich, Germany.

[e] Asklepios Fachkliniken München-Gauting, Robert-Koch-Allee 2, 82131 Gauting, Germany

[f] Medizinische Klinik und Poliklinik V, Klinikum der Ludwig-Maximilians-Universität, Marchioninistraße 15, 81377 Munich, Germany; Member of the German Center of Lung Research (DZL)

[g] Present address: Pulmonary and Critical Care Medicine University, Colorado Anschutz Medical Campus, Denver, Colorado, United States of America

[#] JM-P and TB contributed equally to this work

--- SUPPLEMENTARY INFORMATION ---

Supplementary Tables S1 and S2

Supplementary Figures S1-S19

Supplementary Table S1: Primer table for qRT-PCR analysis, in alphabetical order for gene names. Primers were synthesized by MWG Eurofins (Ebersberg, Germany).

Target	**Forward primer** (5′-3′)	**Reverse primer** (5′-3′)
BGN	ATGACTTCAAGGGTCTCC	TGGTTCTTGGAGATGTAGA
COL6A1	GACGCACTCAAAAGCA	ATCAGGTACTTATTCTCCTTCA
COL6A2	AGAAAGGAGAGCCTGCGGAT	AGGTCTCCCTCACGTAGGTC
COL6A3	CTCTACCGAGCCCAGGTGTT	ATGAGGGTGCGAACGTACTG
COL8A1	GTATGGCAAAGAGTATCCA	GTAAACTGGCTAATGGTATTT
CTSK	GTTACTCCTGTCAAAAATCAG	TCATTCTCAGACACACAATC
DHX8	TGACCCAGAGAAGTGGGAGA	ATCTCAAGGTCCTCATCTTCTTCA
FGF2	ACCCTCACATCAAGCTAC	AAGAAACACTCATCCGTAA
GDF15	CTACGAGGACCTGCTAA	ACTTCTGGCGTGAGTATC
GPC1	GACTATTGCCGAAATGTG	ATGTACCCCAGAACTTGTC
HTRA1	TTGTTTCGCAAGCTTCCGTT	ACGTGGGCATTTGTCACGAT
LAMA4	CAAGAACTGTGCAGTGTG	AGACGCACTTATCACAGC
LAMB2	CCGATATTTCTCCTATGACT	ATGGCTCAATCTCTGAGTAG
LGALS1	AGCAACCTGAATCTCAAA	CAGGTTGTTGCTGTCTTT
LTBP2	CTGACAAGGGTGACTCTC	CACTTGTTCTTCCTGTATCTC
PLOD2	GATCTGGTTGTCATGTTTACT	TGTCTGCTAGTCTTTTATCTG
SEMA7A	TGTTCCACTCTAAATACCACT	CCCCTGTCTGTAGTTAGGTA
THSD4	ATCTTGTAACCCTCAGGAC	GCGGTCTTGTAGTAGTTGTA

Supplementary Table S2: Primary antibodies used in the different applications. Secondary HRP-linked antibodies were from GE Healthcare Life Sciences (Freiburg, Germany). WB, Western Blot; IF, immunofluorescent staining

Target	Antibody	Provider	Application
ACTA2	mouse monoclonal anti-ACTA2	Sigma Aldrich, Louis, MO, USA	IF
ACTB	HRP-conjugated anti-ACTB	Sigma Aldrich, Louis, MO, USA	WB
BGN	mouse monoclonal anti-BGN	Santa Cruz, Dallas, USA	WB
CATK	rabbit polyclonal anti-CATK	Abcam, Cambridge, UK	WB
COL6A1	mouse monoclonal anti-COL6A1	Santa Cruz, Dallas, USA	WB
GDF15	goat polyclonal anti-GDF15	R&D Systems, Minneapolis, USA	WB
LAMA4	mouse monoclonal anti-LAMA4	Santa Cruz, Dallas, USA	WB
LAMB2	mouse monoclonal anti-LAMB2	Santa Cruz, Dallas, USA	WB
PLOD2	mouse monoclonal anti-PLOD2	R&D Systems, Minneapolis, USA	WB
SEMA7A	mouse monoclonal anti-SEMA7A	Santa Cruz, Dallas, USA	WB

For **supplementary Table S3**, please refer to separate Excel File.

Supplementary Figure S1: *In vitro* model used for this study. Primary human lung fibroblasts cultured in presence of TGF-β1 and 2-phosphoascorbate undergo myofibroblast differentiation and consistently increase expression and secretion of collagens, in particular collagen I [1, 2]. (A) Representative immunofluorescent images show that treatment of phLFs with 2 ng/ml TGF-β1 results in cell hypertrophy, increased expression of α-smooth muscle actin (α-SMA, red), and generation of stress fibers, all characteristics of the myofibroblast. Scale bar 50 μm. (B) Transcript fold changes (2 ng/ml TGF-β1 vs. ctrl) for COL1A1 (encoding the α1-chain of type I collagen, n=12), fibronectin (FN1, n=12), and ACTA2 (encoding α-SMA, n=4). (C) Representative Western Blot analysis shows increased protein levels of type I collagen and α-SMA in response to 2 ng/ml TGF-β1. (D) Sircol assay shows increased levels of total secreted collagen (n=14). (E) Quantification of miR-29 expression reveals decreased levels of miR-29b in response to 2 ng/ml TGF-β1 (n=5).

Supplementary Figure S1

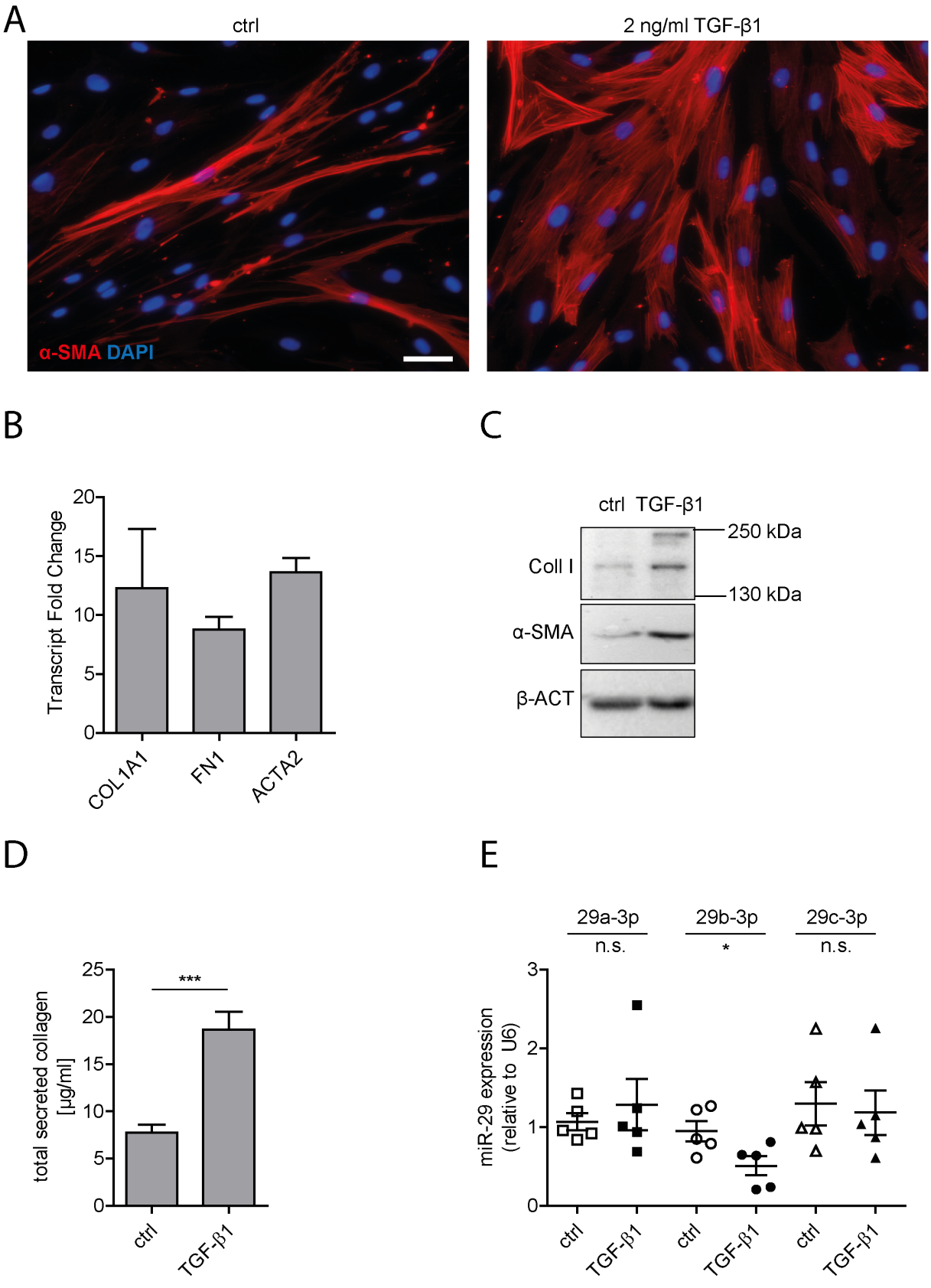

Supplementary Figure S2: Correlation analysis of (**A**) the here presented *in vitro* data set and an ECM data set from the mouse model of bleomycin-induced lung fibrosis [3] and (**B**) the same mouse model data set with a human ECM data set derived from interstitial lung disease patients [4]. Names are given for proteins that deviate by a log2 ratio > 1 from the perfect correlation. Collagens are given in red, ECM glycoproteins in green, proteoglycans in blue, ECM regulators in purple, ECM-affiliated proteins in brown, and secreted factors in black.

Supplementary Figure S2

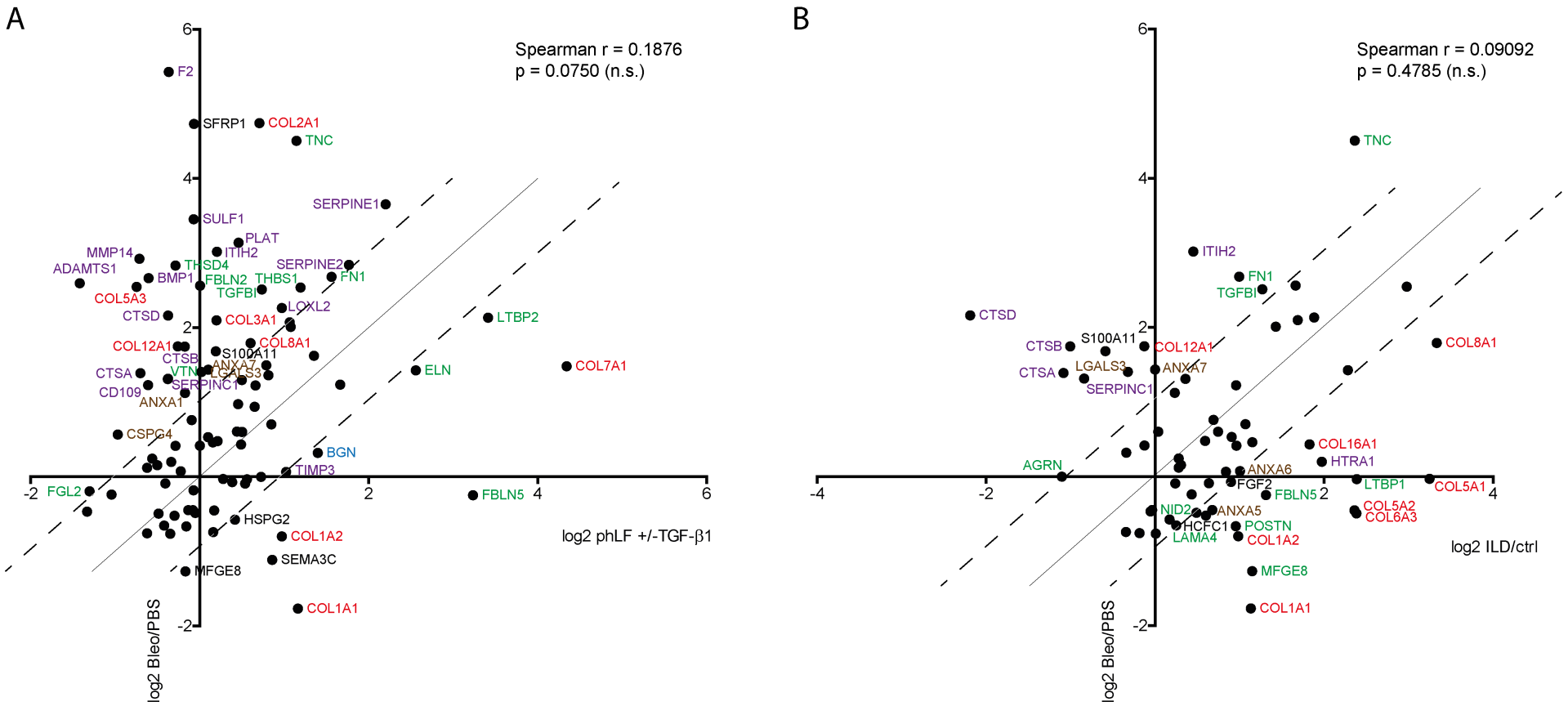

Supplementary Figures S3-S19: Peptide spectrum matches (PSMs) of 11 3-hydroxyproline and 6 O-glycosylation sites in human COL1A1 chain. PSMs were annotated using pLABEL [5].

m/z= 667.8230^{+2}

PSM showing the identification of 3-HyP^{426}

Human col1a1 chain

Q-Exactive HF, HCD Fragmentation

S3

^{416}G P S G P Q G P G G **P**$_{+16}$ P$_{+16}$ G P$_{+16}$ K^{430}

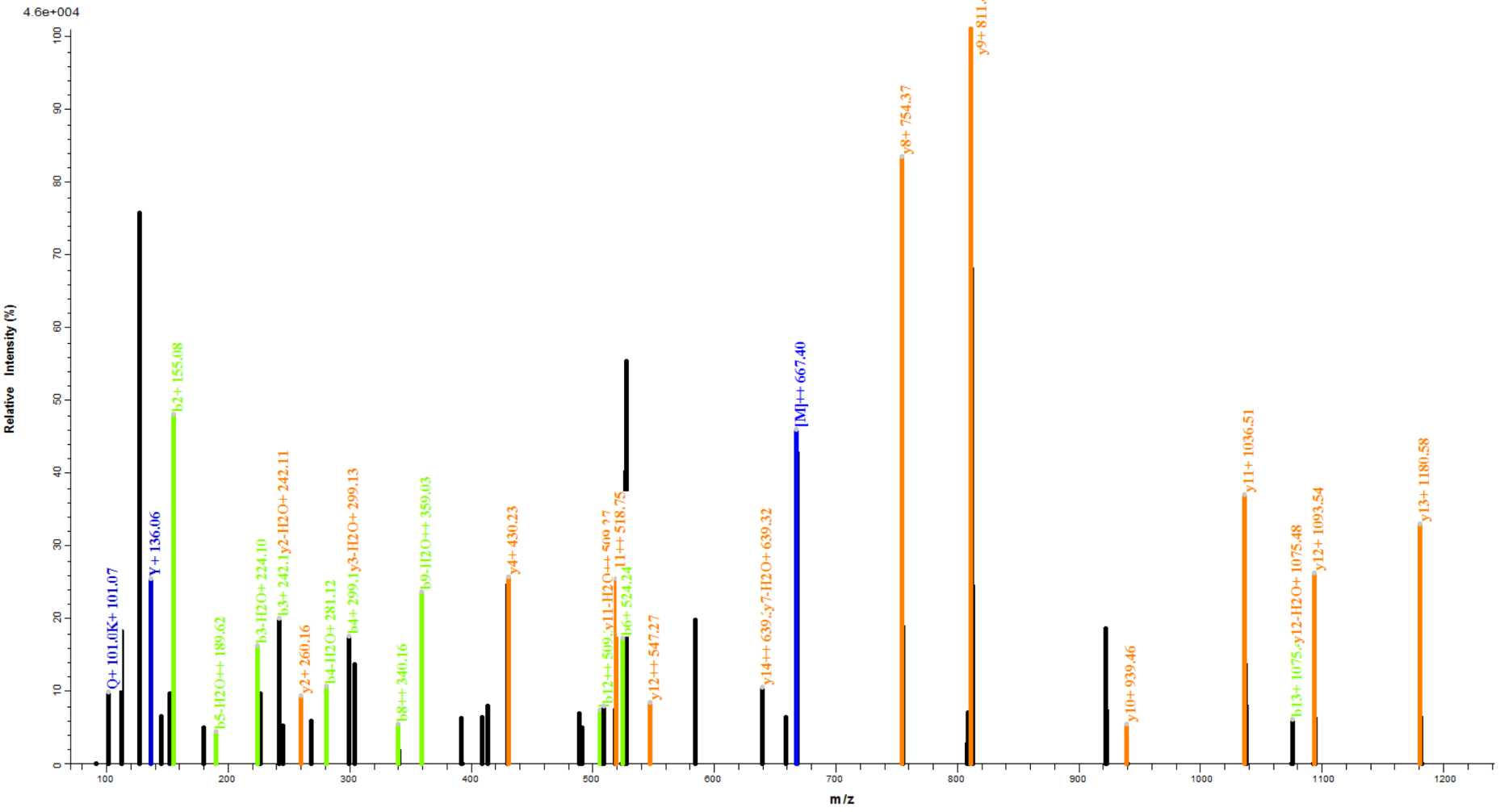

m/z= 691.6630^{+3}

PSM showing the identification of 3-HyP^{555,567}

Human col1a1 chain

Q-Exactive HF, HCD Fragmentation

S4

^{553}T G **P**$_{+16}$ P$_{+16}$ G P A G Q D G R P G **P**$_{+16}$ P$_{+16}$ G P P$_{+16}$ G A R^{574}

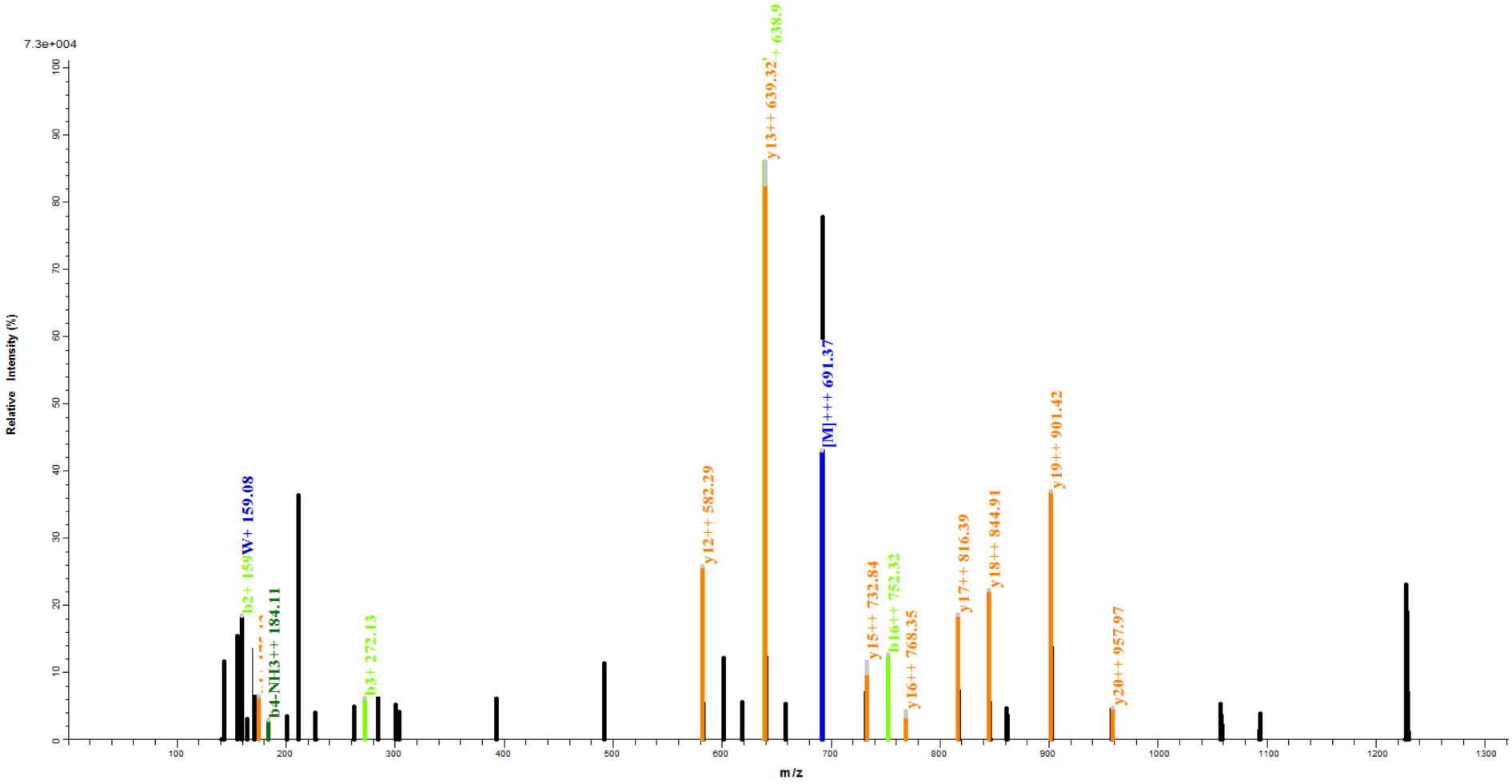

m/z= 561.2893^{+2}

PSM showing the identification of 3-HyP^{690}

Human col1a1 chain

Q-Exactive HF, HCD Fragmentation

S5

^{686}G V Q G **P**$_{+16}$ P$_{+16}$ G P A G P R^{697}

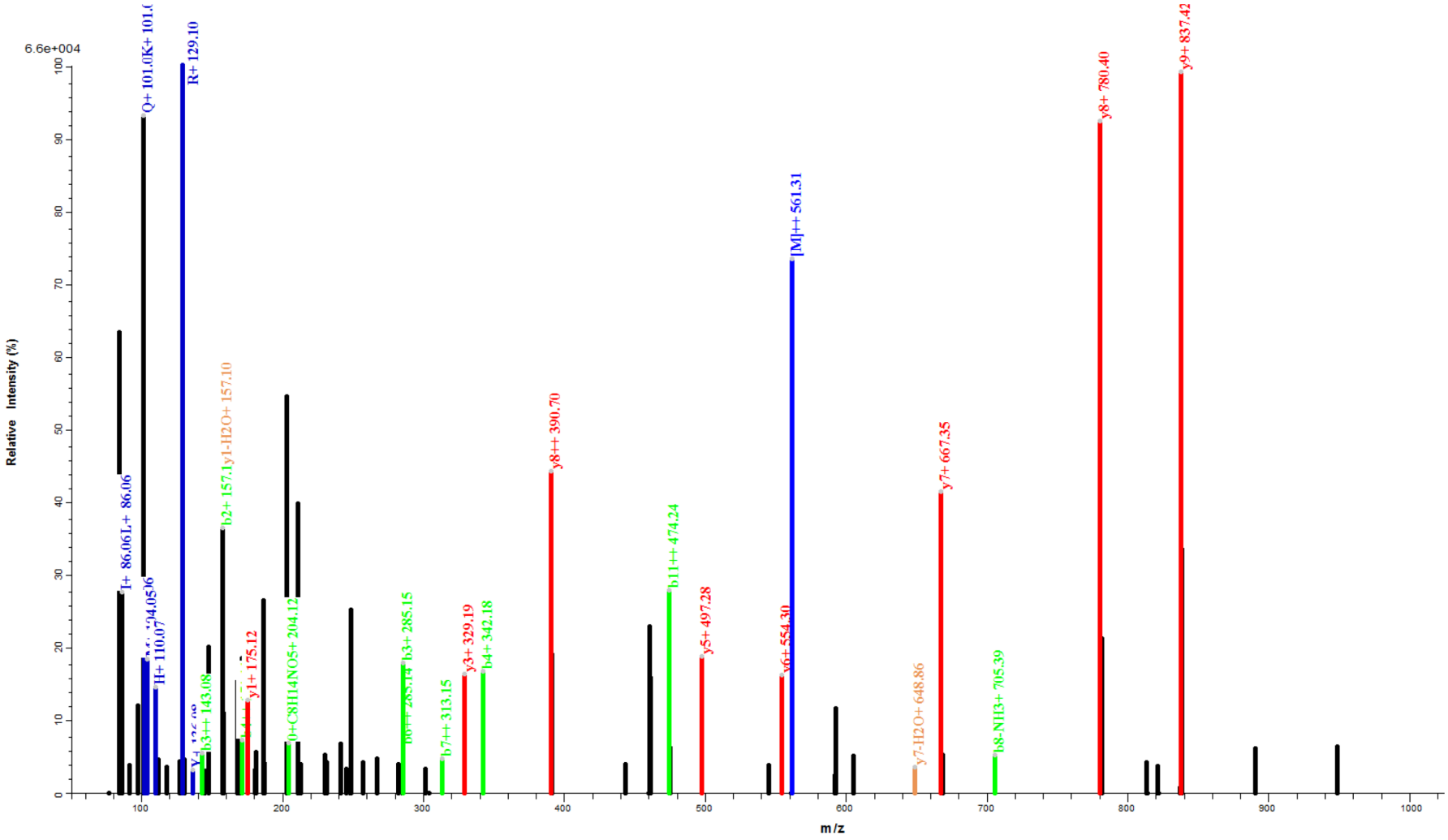

m/z= 930.9402^{+2}

PSM showing the identification of 3-HyP^{885,894,897}

Human col1a1 chain

Q-Exactive HF, HCD Fragmentation

S6

883 V G **P**$_{+16}$ P$_{+16}$ G P S G N A G **P**$_{+16}$ P$_{+16}$ G **P**$_{+16}$ P$_{+16}$ G P A G K 903

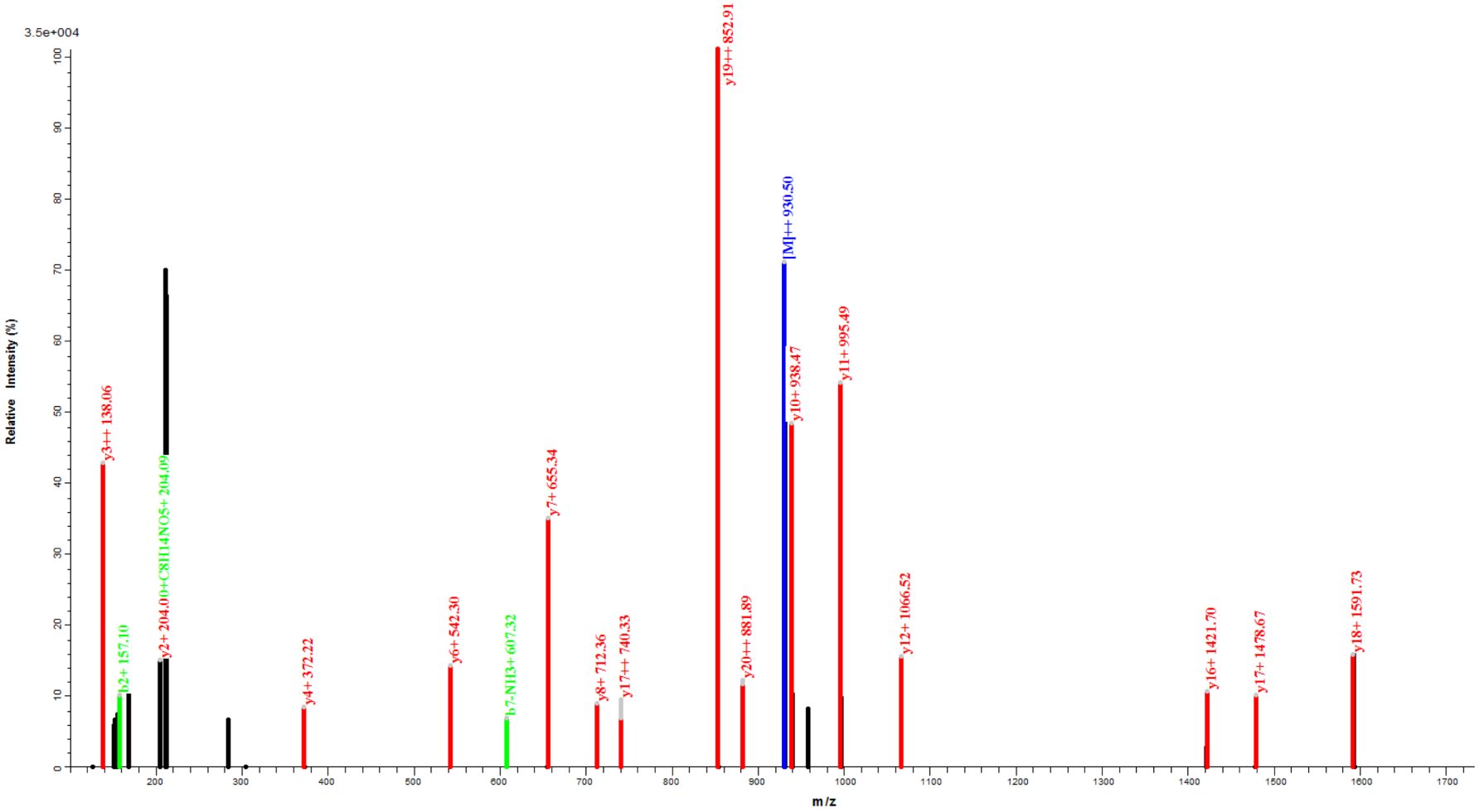

m/z= 1369.1249^{+2} PSM showing the identification of 3-HyP^{1119,1122} Human col1a1 chain

S7

Q-Exactive HF, HCD Fragmentation

^{1112}G F S G L Q G **P**$_{+16}$ P$_{+16}$ G **P**$_{+16}$ P$_{+16}$ G S P$_{+16}$ G E Q G P S G A S G P A G P R^{1141}

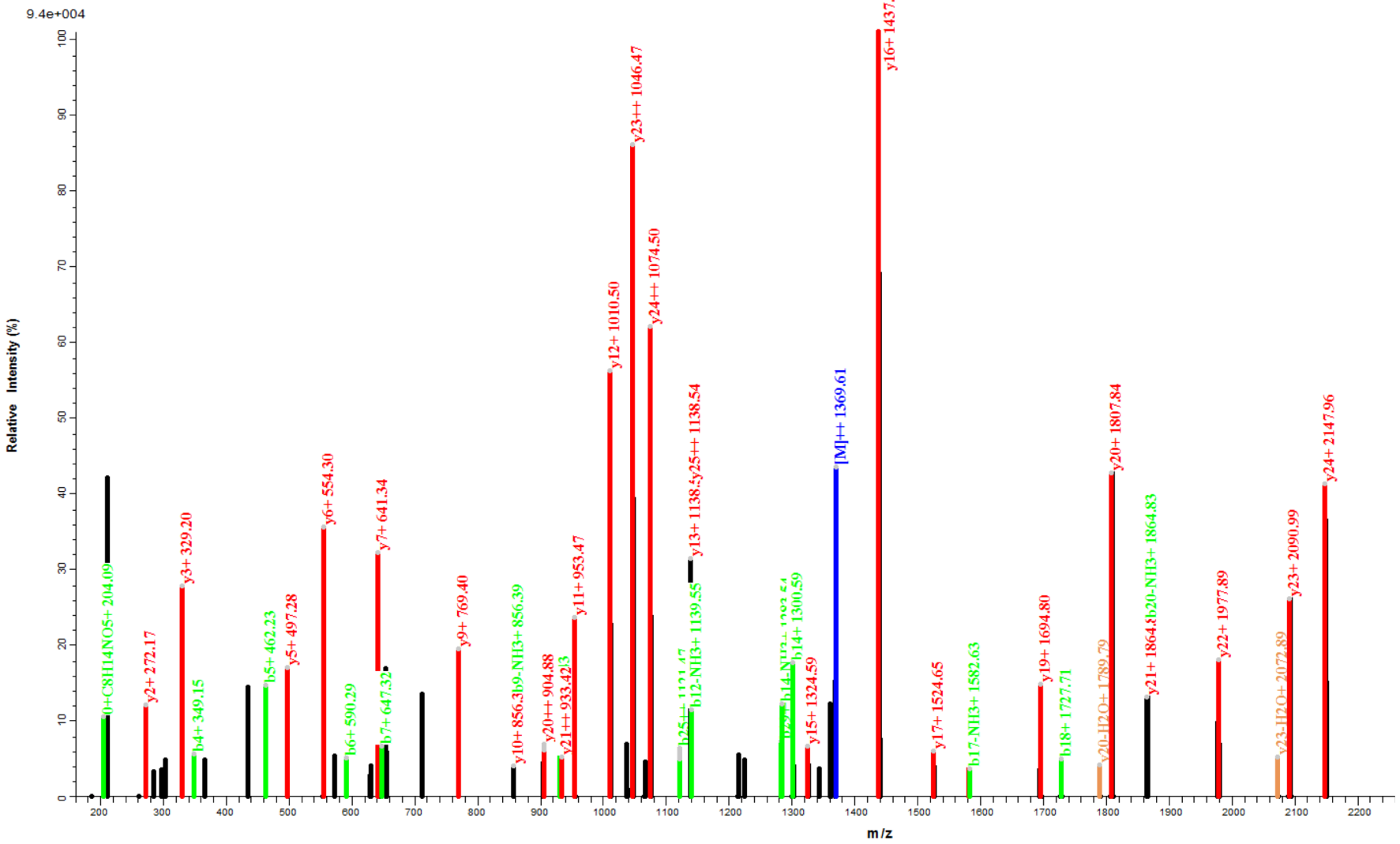

m/z= 781.4037^{+2} PSM showing the identification of 3-HyP^{1164} Human col1a1 chain

Q-Exactive HF, HCD Fragmentation

S8

1158 D G L N G L P$_{+16}$ G P I G **P**$_{+16}$ P$_{+16}$ G P R 1168

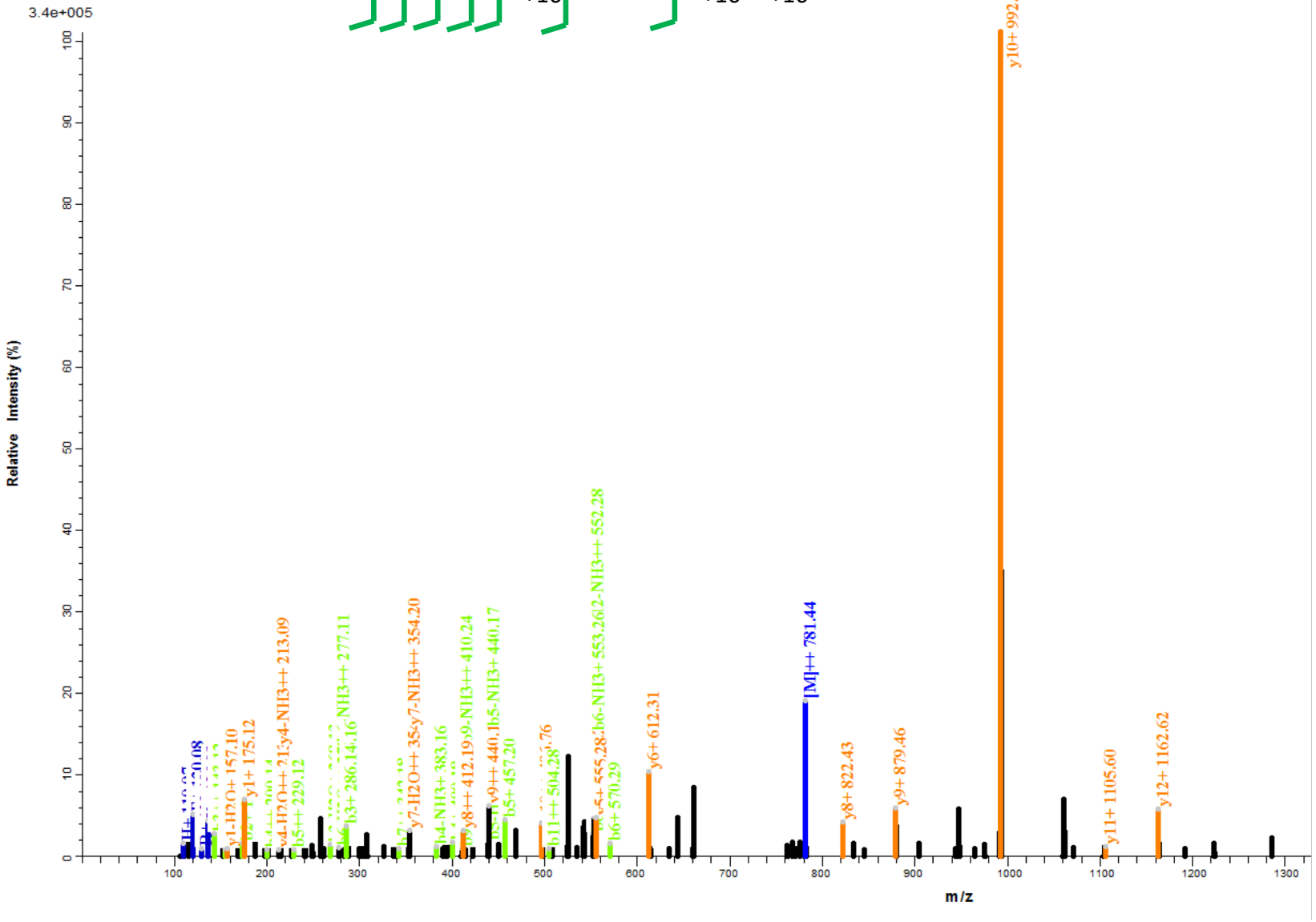

m/z= 1253.9178^{+3}

PSM showing the identification of 3-HyP^{1179}

Human col1a1 chain

Q-Exactive HF, HCD Fragmentation

S9

1171 T G D A G P V G **P**$_{+16}$ P$_{+16}$ G P P$_{+16}$ G P P$_{+16}$ G P P$_{+16}$ G P$_{+16}$ P S A G F D F S F L P Q P P$_{+16}$ Q E K 1208

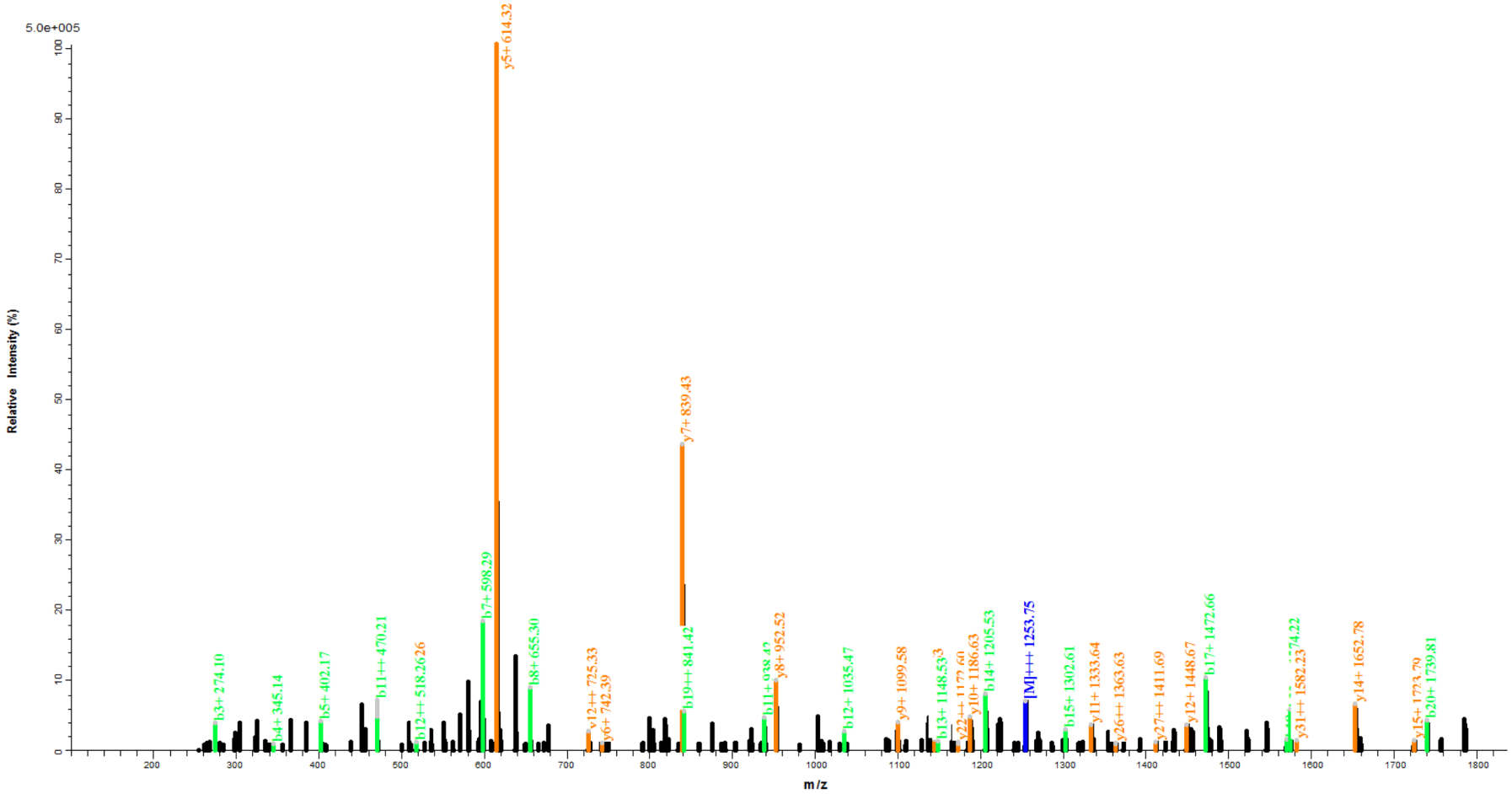

PSM showing the identification of Glucosylgalactosyl-hydroxylysine[265]

m/z= 910.9429^{+2}

Human col1a1 chain

Q-Exactive HF, HCD Fragmentation

S10

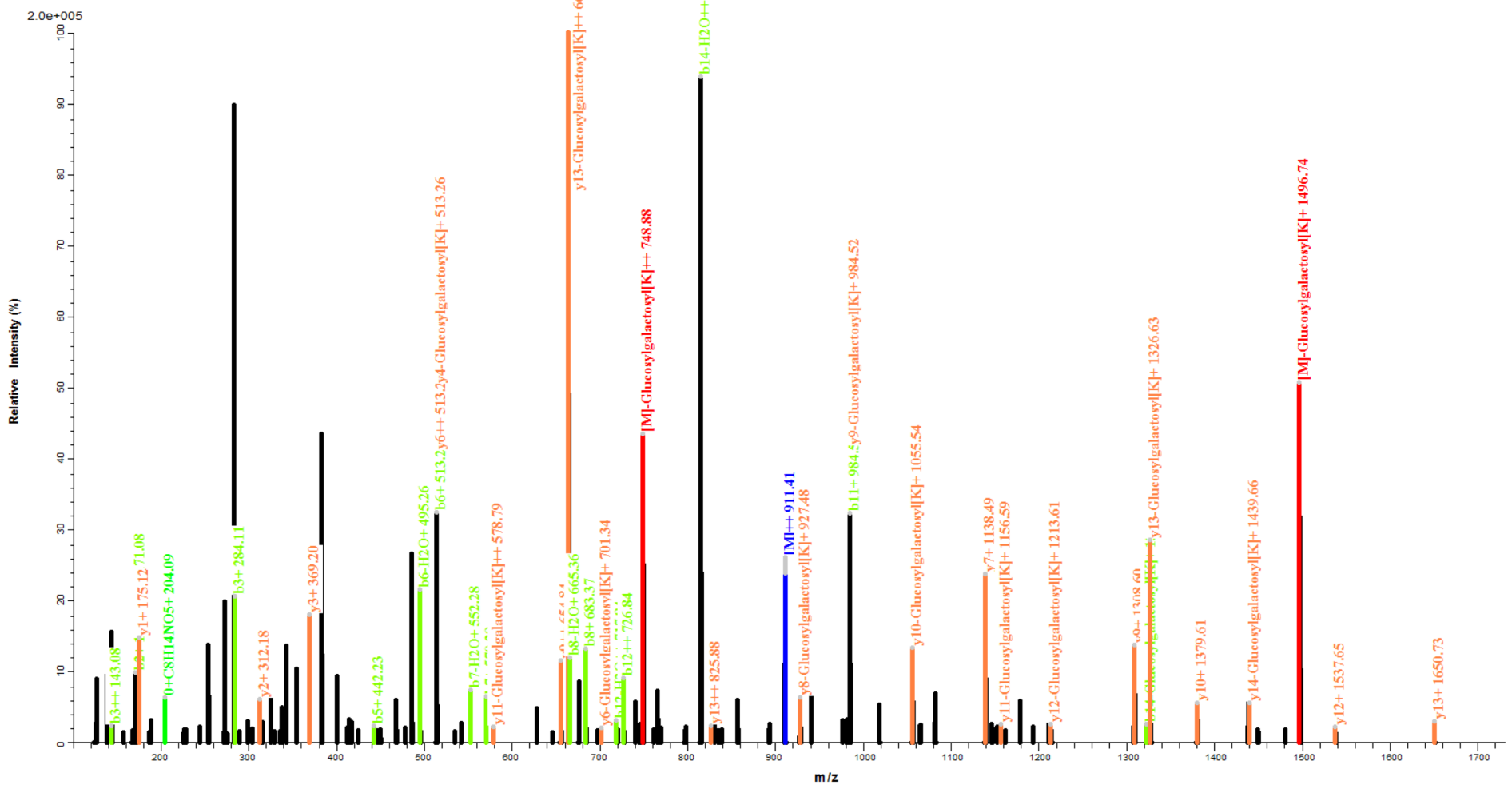

PSM showing the identification of Galactosyl-hydroxylysine[277]

m/z= 898.4209^{+2}

Human col1a1 chain

Q-Exactive HF, HCD Fragmentation

S11

^{269}G F S G L D G A **K**$_{+178}$ G D A G P A G P K$_{+16}^{286}$

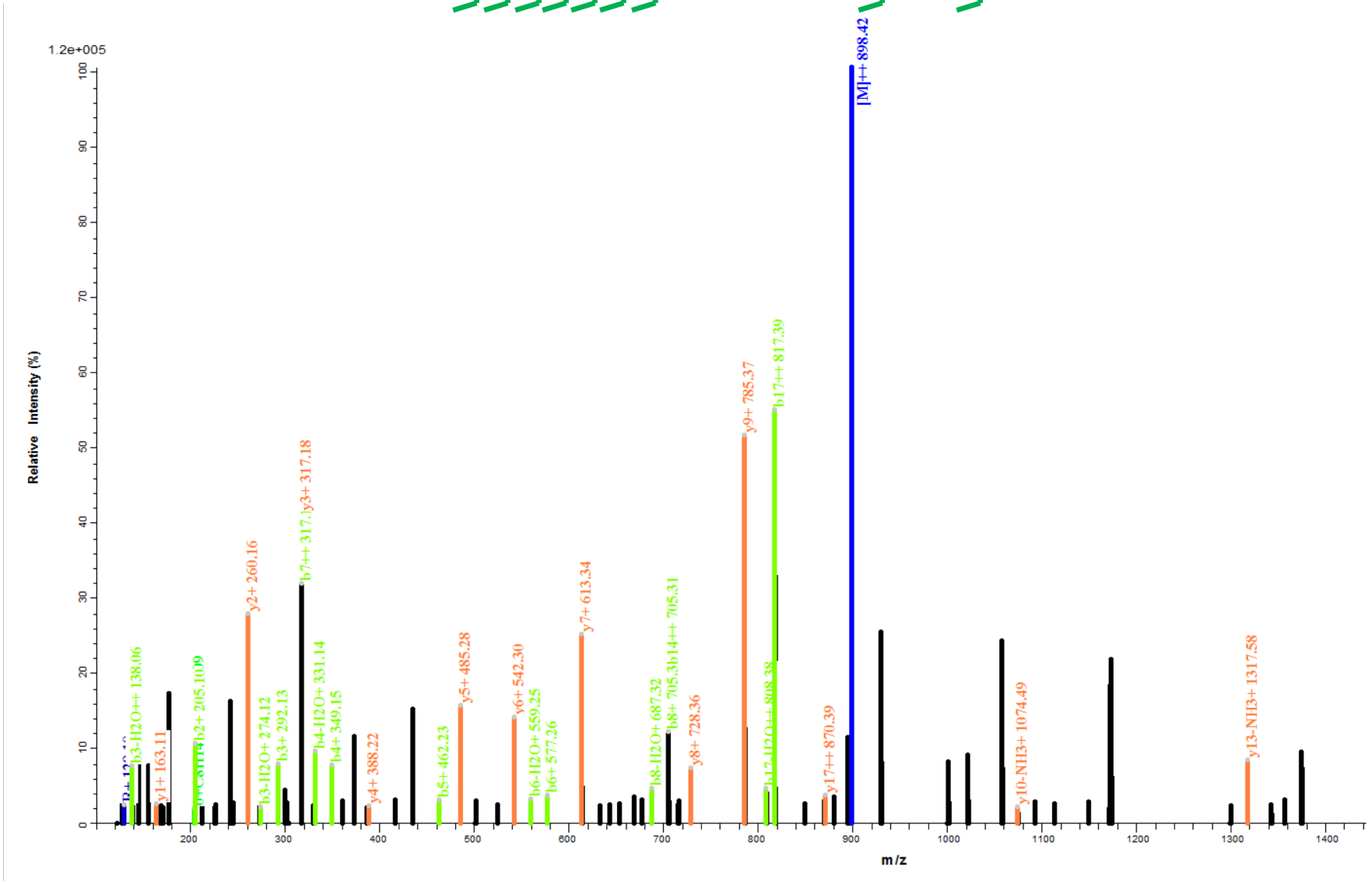

PSM showing the identification of Glucosylgalactosyl-hydroxylysine^{277}

m/z= 979.4489^{+2}

Human col1a1 chain

Q-Exactive HF, HCD Fragmentation

S12

^{269}G F S G L D G A **K**$_{+340}$ G D A G P A G P K$^{286}_{+16}$

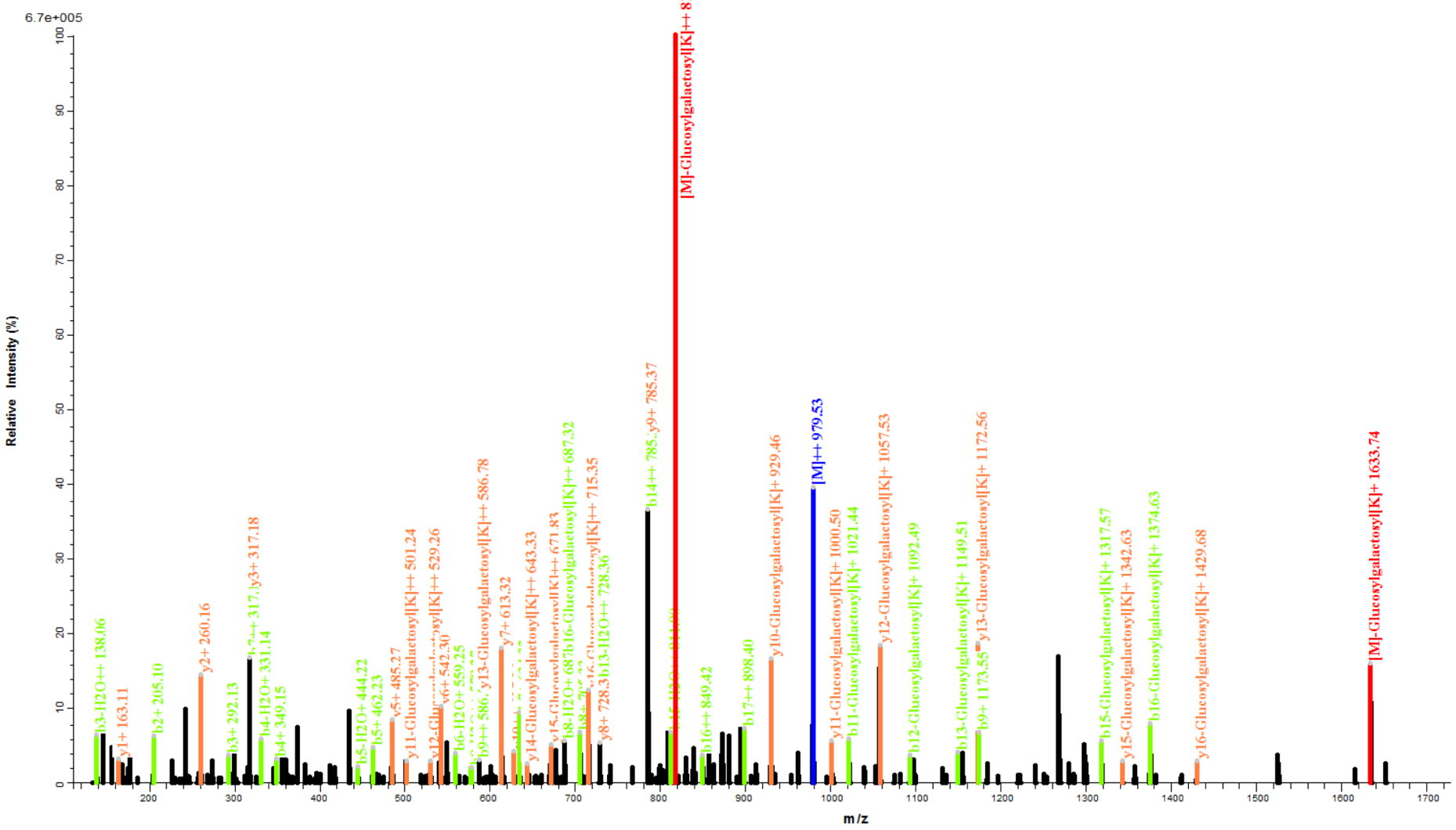

PSM showing the identification of Galactosyl-hydroxylysine[448]

Human col1a1 chain

m/z= 852.3983[+3]

Q-Exactive HF, HCD Fragmentation

S13

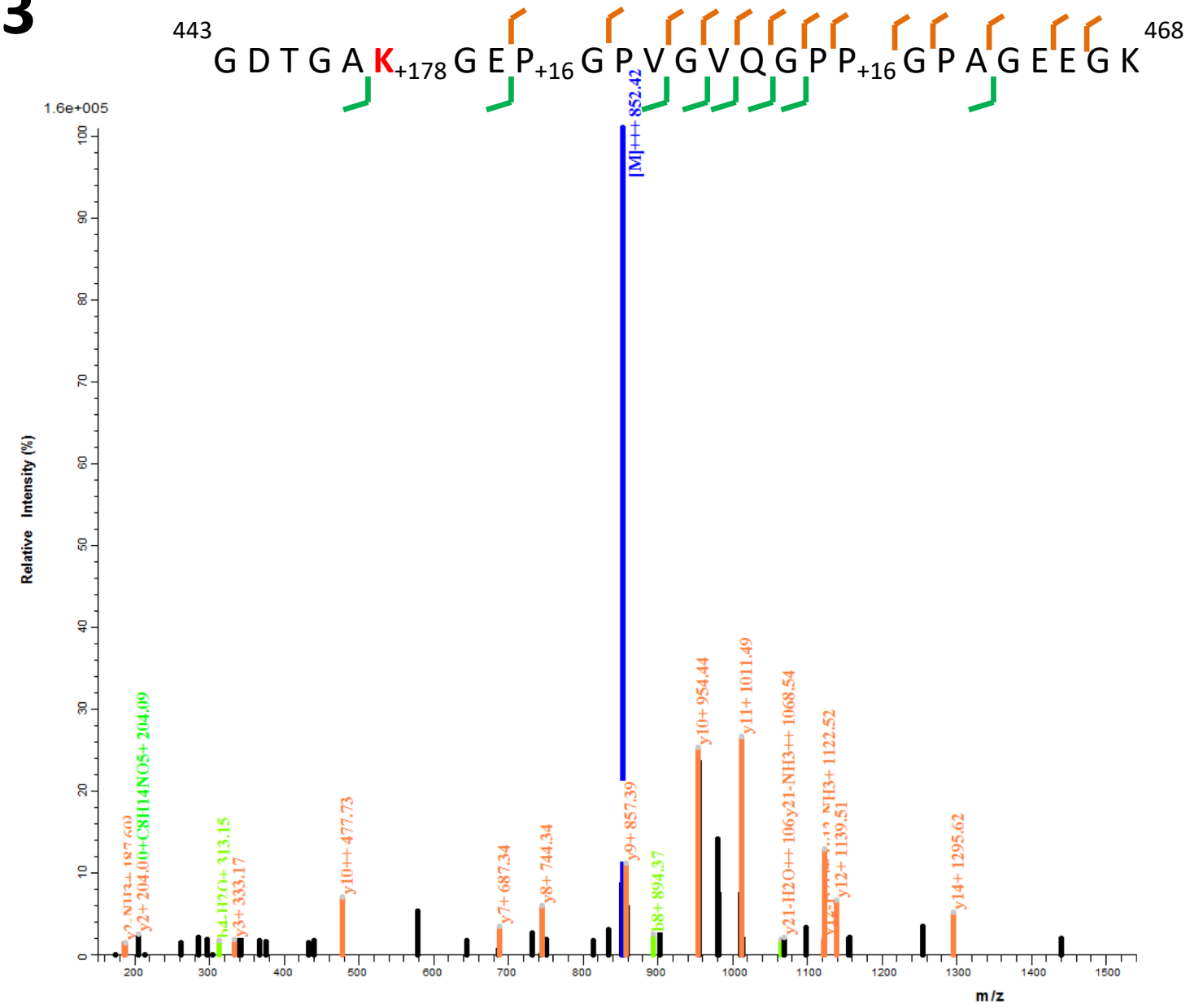

PSM showing the identification of Glucosylgalactosyl-hydroxylysine[448]

m/z= 906.4133^{+3}

Human col1a1 chain

Q-Exactive HF, HCD Fragmentation

S14

443 G D T G A **K**$_{+340}$ G E P$_{+16}$ G P V G V Q G P P$_{+16}$ G P A G E E G K 468

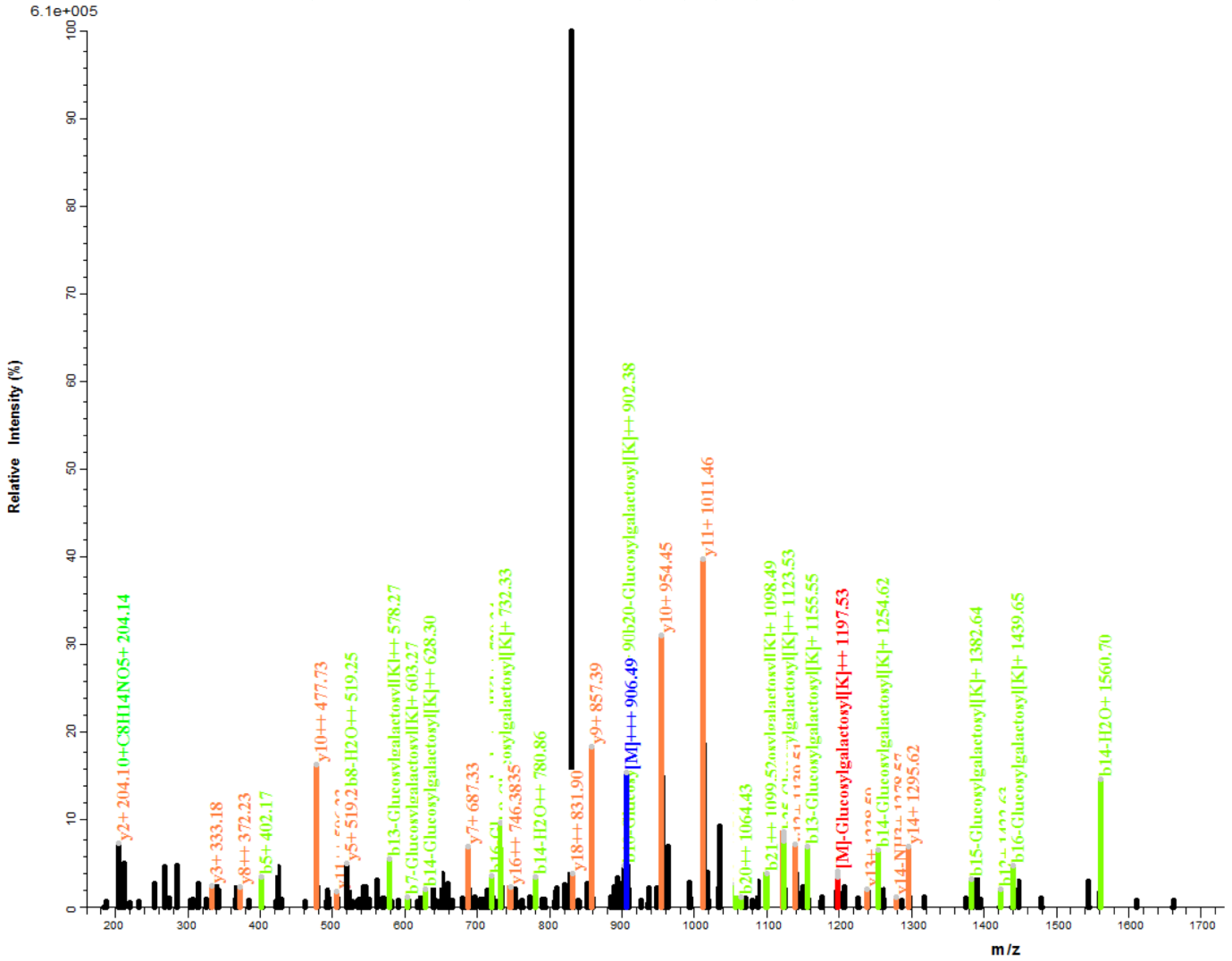

PSM showing the identification of Galactosyl-hydroxylysine^{520}

Human col1a1 chain

m/z= 650.3116^{+4}

Q-Exactive HF, HCD Fragmentation

S15

^{512}G S P G P A G P$_{+16}$ **K**$_{+178}$ G S P$_{+16}$ G E A G R P$_{+16}$ G E A G L P$_{+16}$ G A K^{538}

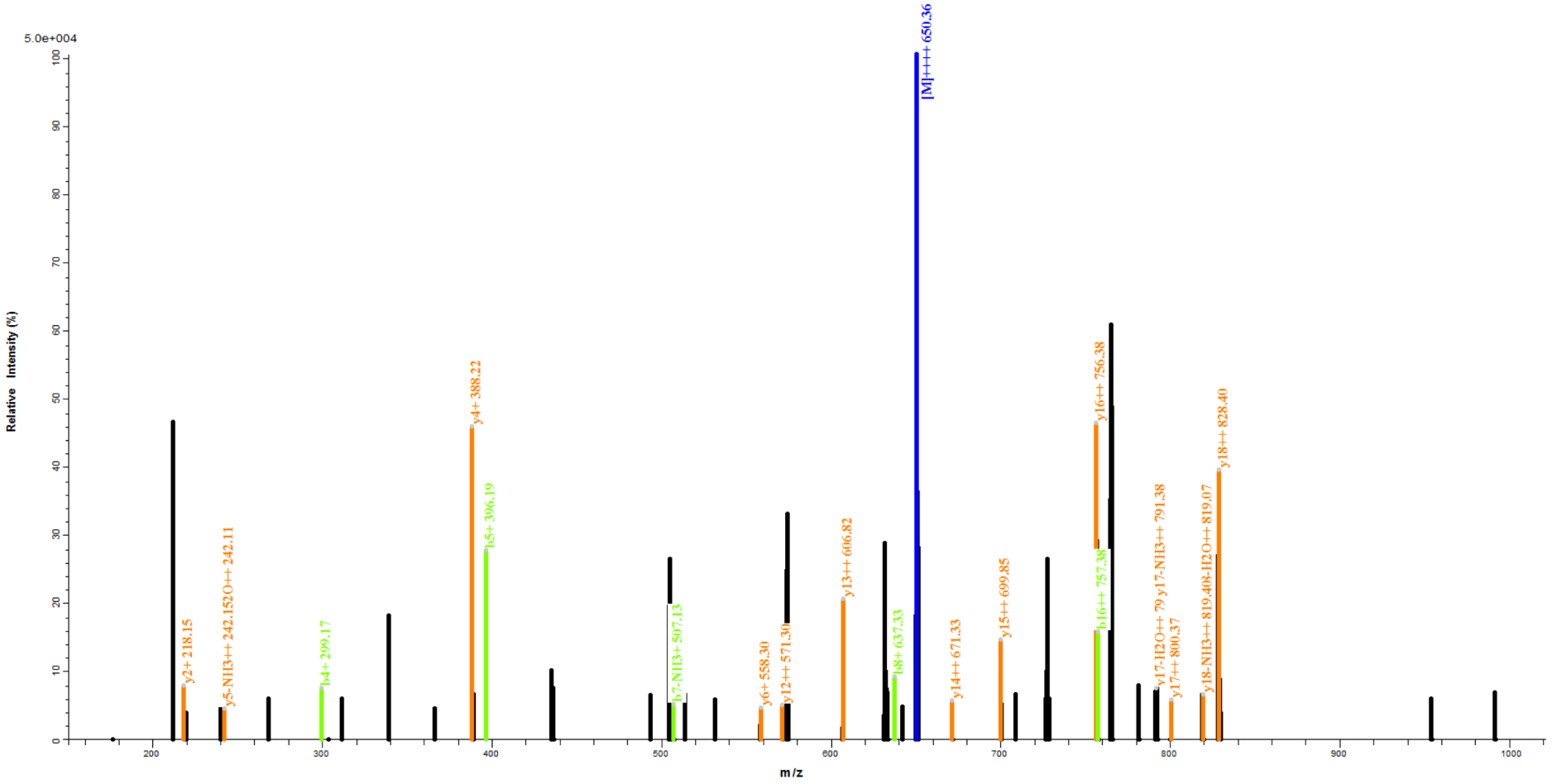

PSM showing the identification of Glucosylgalactosyl-hydroxylysine^{520}

m/z= 920.7651^{+3}

Human col1a1 chain

Q-Exactive HF, HCD Fragmentation

S16

^{512}G S P G P$_{+16}$ A G P **K**$_{+340}$ G S P G E A G R P$_{+16}$ G E A G L P$_{+16}$ G A K$_{+16}$ ^{538}

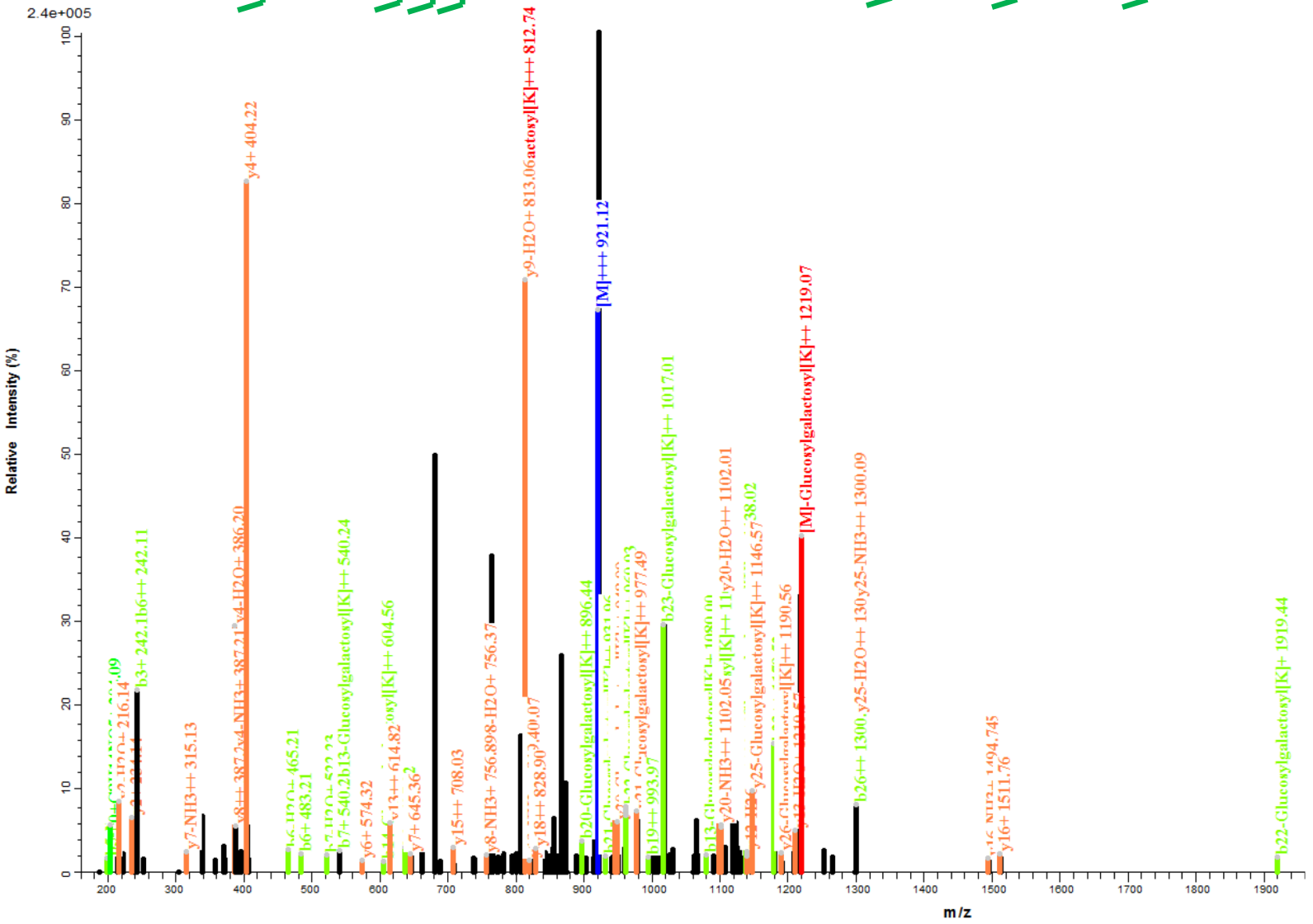

PSM showing the identification of Galactosyl-hydroxylysine[586]

Human col1a1 chain

m/z= 674.9879^{+3}

Q-Exactive HF, HCD Fragmentation

S17

^{575}G Q A G V M G F P G P$_{+16}$ **K**$_{+178}$ G A A G E P$_{+16}$ G K ^{594}

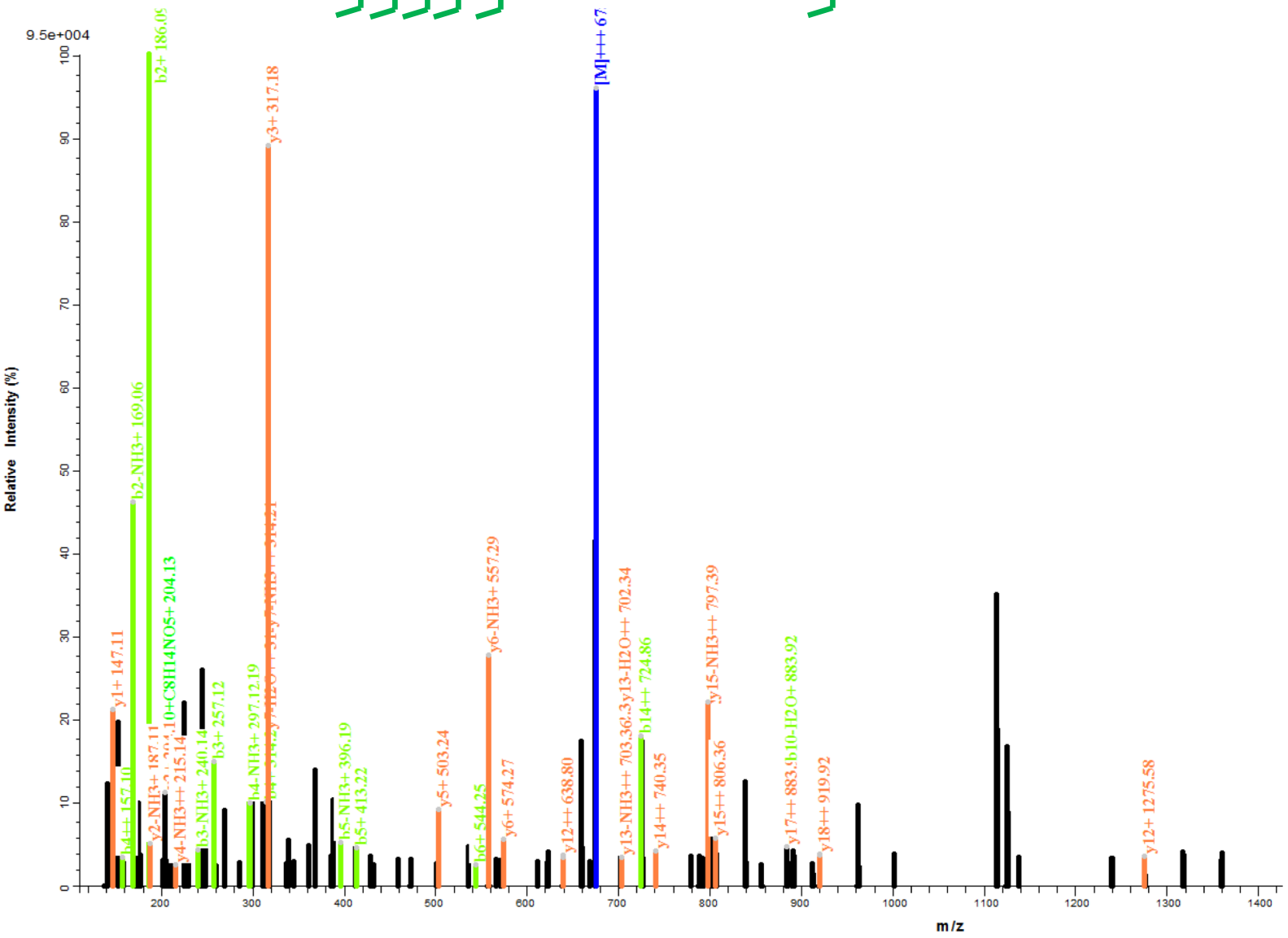

PSM showing the identification of Glucosylgalactosyl-hydroxylysine[586]

m/z= 729.0048[+3]

Human col1a1 chain

Q-Exactive HF, HCD Fragmentation

S18

575 G Q A G V M G F P+16 G P **K**+340 G A A G E P+16 G K 594

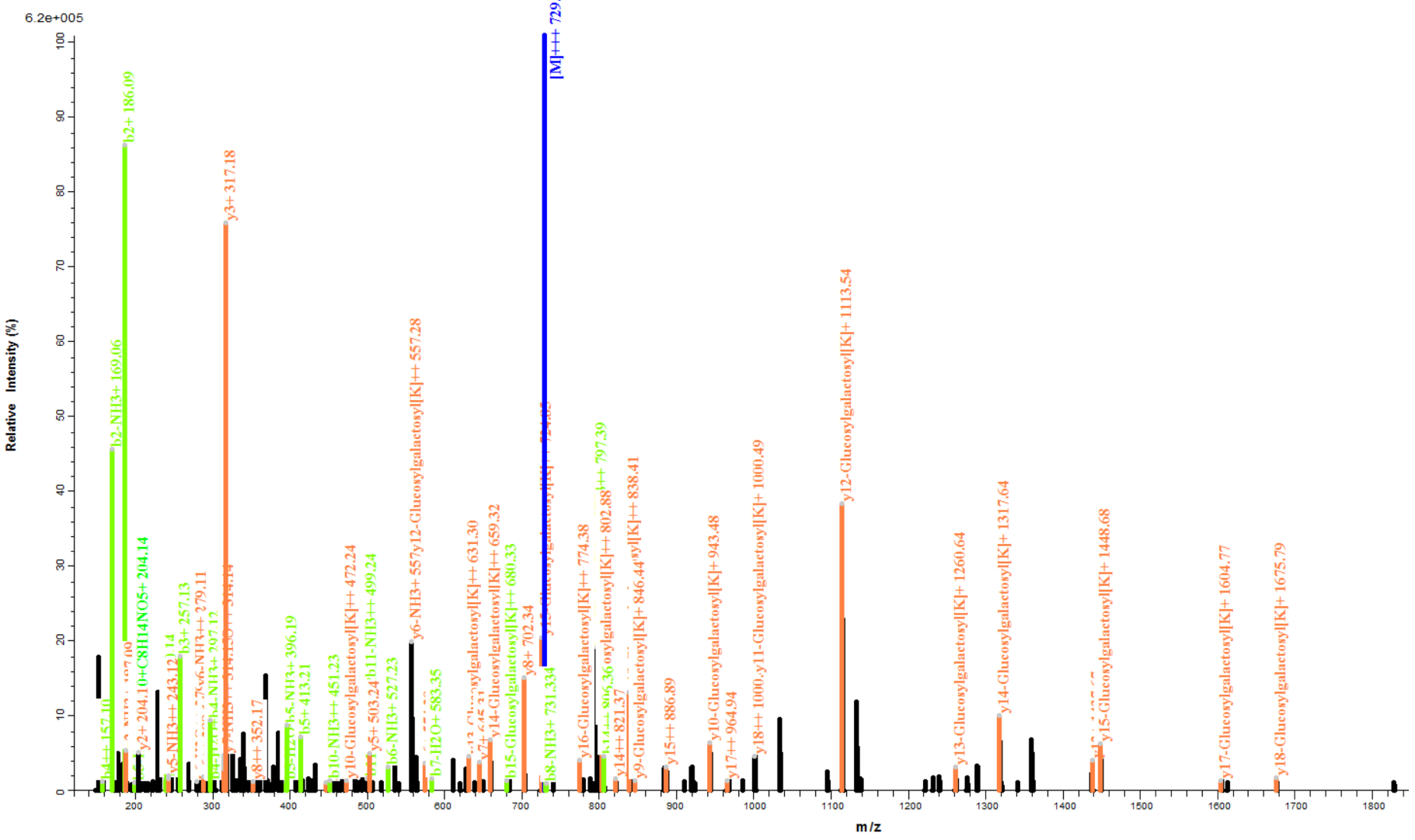

PSM showing the identification of Glucosylgalactosyl-hydroxylysine[862]

Human col1a1 chain

m/z= 963.8028[+3]

Q-Exactive HF, HCD Fragmentation

S19

836 G D A G P P G P A G P A G P A G P P+16 G P I G N V G A P+16 G A **K**+340 G A R 865

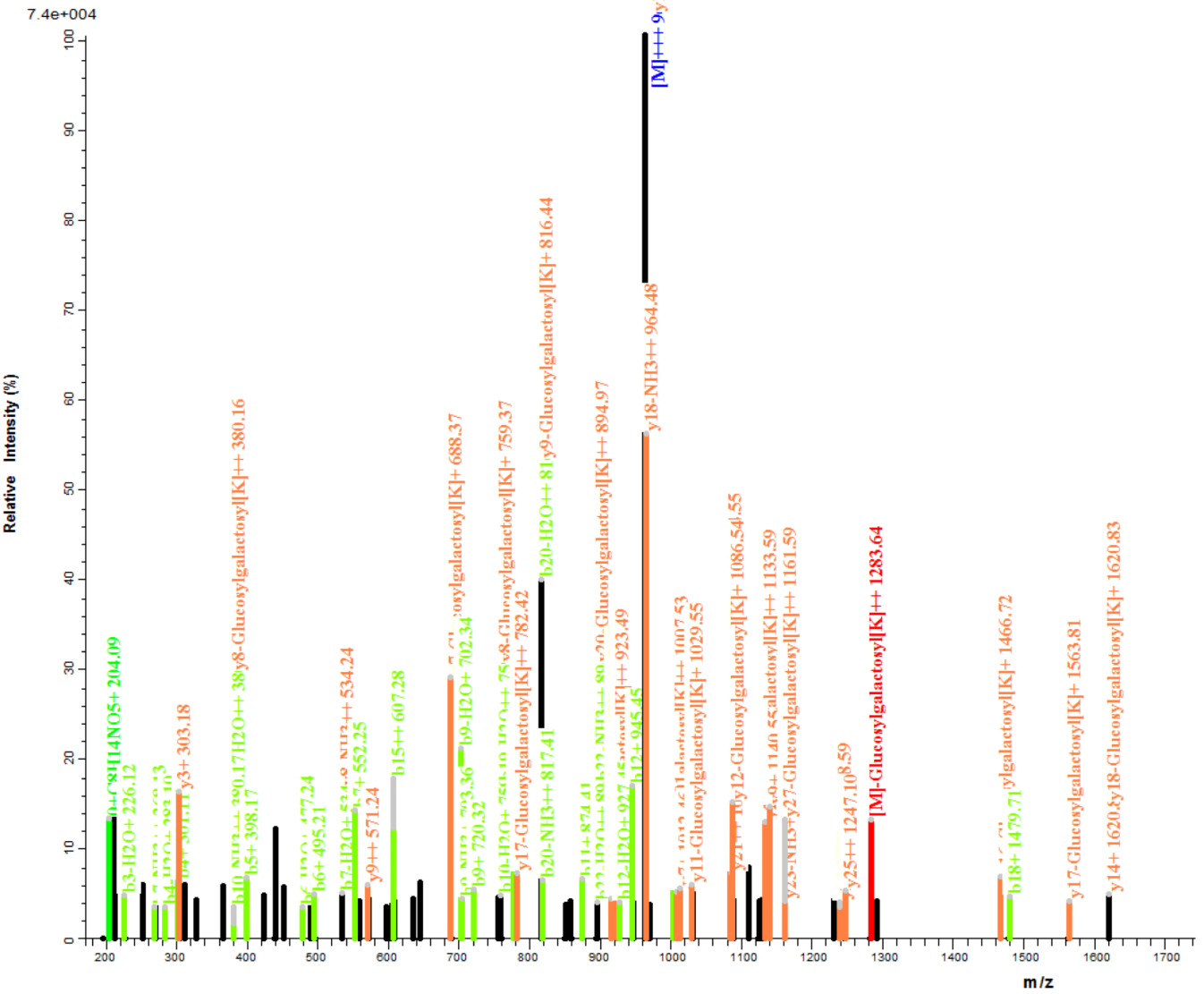

References

[1] L. Knüppel, Y. Ishikawa, M. Aichler, K. Heinzelmann, R. Hatz, J. Behr, A. Walch, H.P. Bächinger, O. Eickelberg, C.A. Staab-Weijnitz, A Novel Antifibrotic Mechanism of Nintedanib and Pirfenidone. Inhibition of Collagen Fibril Assembly, Am. J. Respir. Cell Mol. Biol. 57(1) (2017) 77-90.
[2] C.A. Staab-Weijnitz, I.E. Fernandez, L. Knüppel, J. Maul, K. Heinzelmann, B.M. Juan-Guardela, E. Hennen, G. Preissler, H. Winter, C. Neurohr, R. Hatz, M. Lindner, J. Behr, N. Kaminski, O. Eickelberg, FK506-binding Protein 10 is a Potential Novel Drug Target for Idiopathic Pulmonary Fibrosis, Am. J. Respir. Crit. Care Med. (2015).
[3] H.B. Schiller, I.E. Fernandez, G. Burgstaller, C. Schaab, R.A. Scheltema, T. Schwarzmayr, T.M. Strom, O. Eickelberg, M. Mann, Time- and compartment-resolved proteome profiling of the extracellular niche in lung injury and repair, Mol. Syst. Biol. 11(7) (2015) 819.
[4] H.B. Schiller, C.H. Mayr, G. Leuschner, M. Strunz, C. Staab-Weijnitz, S. Preisendorfer, B. Eckes, P. Moinzadeh, T. Krieg, D.A. Schwartz, R.A. Hatz, J. Behr, M. Mann, O. Eickelberg, Deep Proteome Profiling Reveals Common Prevalence of MZB1-Positive Plasma B Cells in Human Lung and Skin Fibrosis, Am. J. Respir. Crit. Care Med. 196(10) (2017) 1298-1310.
[5] R.X. Sun, M.Q. Dong, C.Q. Song, H. Chi, B. Yang, L.Y. Xiu, L. Tao, Z.Y. Jing, C. Liu, L.H. Wang, Y. Fu, S.M. He, Improved peptide identification for proteomic analysis based on comprehensive characterization of electron transfer dissociation spectra, J. Proteome Res. 9(12) (2010) 6354-67.